

Citation for published version:

Thomas Kopsch, Darragh Murnane, and Digby Symons, 'A personalized medicine approach to the design of dry powder inhalers: Selecting the optimal amount of bypass', *International Journal of Pharmaceutics*, Vol. 529 (1-2): 589-596, August 2017.

DOI:

<https://doi.org/10.1016/j.ijpharm.2017.07.002>

Document Version:

This is the Published Version.

Copyright and Reuse:

© 2017 Elsevier.

This is an Open Access article, distributed under the terms of the Creative Commons Attribution licence (<http://creativecommons.org/licenses/by/4.0/>), which permits unrestricted re-use, distribution, and reproduction in any medium, provided the original work is properly cited.

Enquiries

If you believe this document infringes copyright, please contact the Research & Scholarly Communications Team at rsc@herts.ac.uk



Research paper

A personalized medicine approach to the design of dry powder inhalers: Selecting the optimal amount of bypass



Thomas Kopsch^{a,*}, Darragh Murnane^b, Digby Symons^c

^a University of Cambridge, Department of Engineering, Trumpington Street, CB2 1PZ, UK

^b University of Hertfordshire, Department of Pharmacy, Pharmacology and Postgraduate Medicine, College Lane, AL10 9AB, UK

^c University of Canterbury, Mechanical Engineering Department, Christchurch 8140, New Zealand

ARTICLE INFO

Article history:

Received 19 May 2017

Received in revised form 29 June 2017

Accepted 1 July 2017

Keywords:

Dry powder inhaler

Bypass

Computational fluid dynamics

Optimization

Meta-model

ABSTRACT

In dry powder inhalers (DPIs) the patient's inhalation manoeuvre strongly influences the release of drug. Drug release from a DPI may also be influenced by the size of any air bypass incorporated in the device. If the amount of bypass is high less air flows through the entrainment geometry and the release rate is lower. In this study we propose to reduce the intra- and inter-patient variations of drug release by controlling the amount of air bypass in a DPI. A fast computational method is proposed that can predict how much bypass is needed for a specified drug delivery rate for a particular patient. This method uses a meta-model which was constructed using multiphase computational fluid dynamic (CFD) simulations. The meta-model is applied in an optimization framework to predict the required amount of bypass needed for drug delivery that is similar to a desired target release behaviour. The meta-model was successfully validated by comparing its predictions to results from additional CFD simulations. The optimization framework has been applied to identify the optimal amount of bypass needed for fictitious sample inhalation manoeuvres in order to deliver a target powder release profile for two patients.

© 2017 Elsevier B.V. All rights reserved.

1. Introduction

Dry powder inhalers (DPI) are devices used to deliver drug powder to the pulmonary airways of a patient. In DPIs drug powder is initially stored in an entrainment compartment. Typically, this is a pre-filled and foil sealed 'blister' that is pierced or opened to allow air to flow through. When a patient inhales through the device, the flow of air entrains the powder and delivers it to the lung. Since the patient generates the inhalation airflow him/herself, drug delivery by means of a DPI is inherently variable and highly patient dependent: when a patient generates a strong inhalation flow rate drug is entrained comparably faster. However, for optimal delivery it is desired to design DPIs that can deliver drug to similar pulmonary airways, independent of a patient's ability to use a device. There have been various attempts to improve DPI drug delivery by studying and optimizing different parts of a DPI. For example, these attempts include: (i) numerical optimization of the entrainment compartment of a DPI (Kopsch

et al., 2016a; Zimarev et al., 2013), (ii) experimental investigation of the effect of add-on spacers on de-agglomeration (Ehtezazi et al., 2008) and (iii) numerical investigations into the effect of DPI geometry on powder de-agglomeration (Chen et al., 2013; Coates et al., 2006; Wong et al., 2011a,b, 2010).

Controlling de-agglomeration of drug particles during the entrainment process is necessary to deliver the formulation to the correct pulmonary regions: small particles ($d < 5 \mu\text{m}$) are typically cohesive and thus form large agglomerates ($d > 10 \mu\text{m}$). Such agglomerates are not easily inhalable due to their aerodynamic properties. Good lung deposition requires particle sizes between $0.1 \mu\text{m}$ and $10 \mu\text{m}$ (Heyder, 2004). It is therefore a key requirement for effective drug delivery that agglomerates of particles are broken up in the device during inhalation. Wong et al. evaluated the influence of turbulence (Wong et al., 2010) and impaction (Wong et al., 2011a,b) on de-agglomeration; impaction was found to be most effective.

There is an opportunity to apply numerical techniques, such as computational fluid dynamics (CFD), to the development of DPIs. Multiphase CFD techniques have been successfully applied to predict the entrainment of drug in a DPI (Milenkovic et al., 2014; Tong et al., 2013; Wong et al., 2011b). Consequently, in our previous work, we applied a CFD technique to optimize the entrainment geometry of a DPI (Kopsch et al., 2016a; 2015; Zimarev et al., 2013).

Abbreviations: CFD, computational fluid dynamics; DPI, dry powder inhaler; EE, Eulerian-Eulerian; MDI, metered dose inhaler.

* Corresponding author.

E-mail address: TK434@cam.ac.uk (T. Kopsch).

<http://dx.doi.org/10.1016/j.ijpharm.2017.07.002>

0378-5173/© 2017 Elsevier B.V. All rights reserved.

The optimization objective was to achieve drug dose emission that (A) is independent of the inhalation manoeuvre and (B) targets the dose to a specific pulmonary region in the lung. This optimization objective was achieved by using a multiphase CFD technique to predict the rate of drug release from an entrainment geometry for two different sample inhalation profiles. The predicted rate of drug entrainment was used to calculate the value of a cost function that quantified the optimization objectives (A) and (B). Finally, the entrainment geometry was systematically varied to achieve lower values of the cost function. The result was an optimized DPI entrainment geometry that achieved better performance in terms of the objectives (A) and (B).

Even though some theoretical progress has been made to reduce patient dependence of DPI drug dose delivery, no practical solution is currently on the market. Drug delivery by means of a DPI is still considered less reliable than delivery by other types of inhalers, i.e. nebulizers or metered dose inhalers (MDIs). One reason is that devices are often made to be used by a wide range of patients (a 'one size fits all' approach). In this study, we investigate, by computational method, if a DPI design can be personalized for the patients it is intended to treat. We propose the amount of air bypass as a DPI design factor to control powder entrainment rate when the entrainment geometry design has been 'locked down' and present a fast computational method that can determine the optimal amount of bypass needed to minimize the variability in drug delivery rate between different inhalation manoeuvres of a given patient. The computational method uses measurements of several inhalation profiles of a particular patient to predict the effect of varying the amount of air bypass in a DPI for that patient. We validate the computational method and demonstrate by means of numerical simulations how such a method may be used to achieve the optimization objective, i.e. to target the dose to a specific pulmonary region in the lung. The focus of this work is to develop the computational method, not the design of a new DPI *per se*, since inhaled products are often retro-engineered into existing commercial platform devices. Therefore, the current approach adopts an existing DPI design where other design elements have been locked down (for example, in the generic design shown in Fig. 1), to study the effect of varying of the magnitude of airflow through the bypass channel.

2. Methods

2.1. Concept development

A simple DPI layout may be thought of as an entrainment compartment and a bypass element in parallel, see Fig. 2. When patients inhale through the device, they generate a total flow rate $Q(t)$. The incoming air divides so that a portion of the air flows through the entrainment compartment, where it may entrain drug powder, and the remainder flows through the bypass element. The

flow rates through the entrainment compartment and the bypass element are $Q_{ent}(t)$ and $Q_{bypass}(t)$ respectively.

Note that the inhaled volume of air $V(t)$ is the integral of the total flow rate $Q(t)$ over time.

$$V(t) = \int_0^t Q(t) dt \quad (1)$$

However, $M(t)$, the mass of drug powder released as a function of time t , only depends on the flow rate through the entrainment compartment $Q_{ent}(t)$. In pharmaceutical applications it is important when the drug is released with respect to the total volume of inhaled air V_{tot} , because this determines which pulmonary locations the drug may be able to reach. Drug released early in the tidal inhalation flow can penetrate deeply into the expanding lungs, whereas later released drug will only reach the upper airways. As explained in Kopsch et al. (2016a, 2015), it is convenient to express the mass of released drug M as a fraction x of the scaled volume, where

$$x = \frac{V(t)}{V_{tot}} \quad (2)$$

The relative flow resistances of the entrainment compartment and the bypass element control the amount of air that flows through each part. For example, if the flow resistance of the bypass element is increased then more air will flow through the entrainment compartment. DPIs may be characterized by the bypass ratio

$$r = \frac{Q_{bypass}}{Q_{ent}} \quad (3)$$

If effects due to the presence of the drug powder are neglected this ratio is approximately constant during an inhalation manoeuvre. For most commercially available DPIs the bypass ratio is fixed at manufacture. However, it may be beneficial to adapt this ratio to the patient. A patient who generates a lower total inhalation flow rate may choose a lower ratio r in order to still achieve a good flow rate Q_{ent} through the entrainment compartment.

As an illustration, Fig. 3 shows the influence of r on the timing of drug release: Fig. 3a shows three possible measurements of inhalation flow rate $Q(t)$ through a DPI. Correspondingly, Fig. 3b–d shows the released drug as a function of scaled volume x for low, medium and high amounts of bypass respectively. As indicated a low bypass can achieve an early delivery of drug, while a high bypass achieves a more continuous delivery. The amount of bypass may be 'tuned' to achieve a better match with a desired release profile.

2.2. Development of a meta-model

The goal is to predict $M(x)$, the mass of drug that has left the entrainment part as a function of scaled volume x , for any given

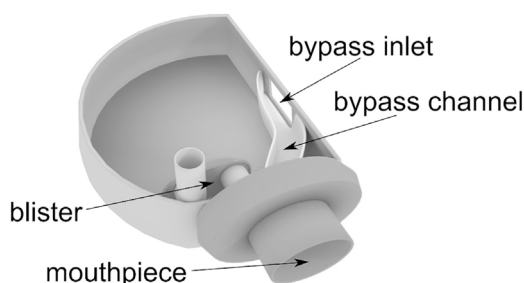


Fig. 1. Simplified drawing of a DPI (top removed) with a blister (powder entrainment compartment) and a fixed bypass. The dimensions of the bypass channel influence the amount of air that bypasses the blister.

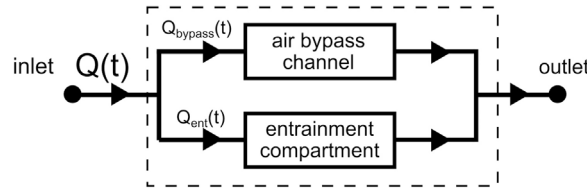


Fig. 2. Schematic layout of a DPI showing a bypass channel (with definable flow resistance) in parallel with an entrainment compartment with defined flow resistance.

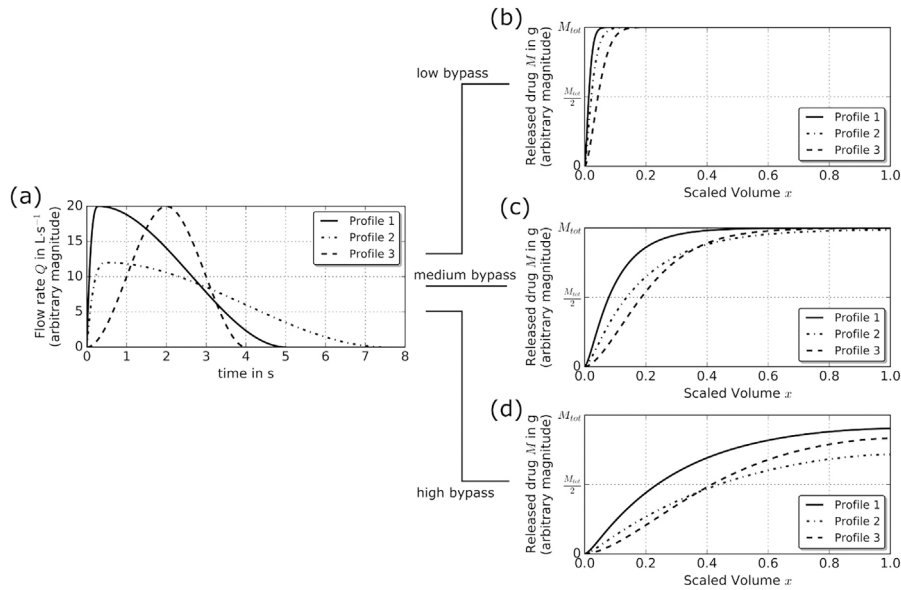


Fig. 3. Idealized representation of inhalation flow rate released drug as a function of scaled volume for different bypasses. Example data for clarification purposes only. (a) Three simulations of inhalation flow rates. Corresponding drug release profiles for: (b) low bypass, (c) medium bypass, and (d) high bypass.

inhalation flow rate profile $Q(t)$. $M(x)$ may be predicted using multiphase CFD simulations. However, high-fidelity CFD simulations tend to be computationally expensive and may not be practical in cases where a large number of predictions are required. For this reason a meta-model was constructed. A meta-model is a simplified model of a complex calculation. A (small) number of computationally expensive simulation results are used to build a lower fidelity model that can predict further results with low computational cost. Here, the meta-model was constructed in the following way. First, a number of high-fidelity (computationally-expensive), two phase CFD simulations of a particular entrainment compartment were conducted to predict $M(t)$, the mass of released drug as a function of time t , for a range of different flow rate profiles

$Q_{ent}(t)$. Second, using the CFD results a meta-model was constructed by interpolating between data points. This meta-model can be used to predict $M(t)$ for further new flow rate profiles for the chosen entrainment geometry.

2.2.1. Computational fluid dynamics approach

A two phase Eulerian–Eulerian (EE) CFD approach was applied to simulate the entrainment of drug powder in the entrainment compartment of a DPI. ANSYS Fluent (ANSYS, 2009) was used to model the transient entrainment of drug formulation when different constant flow rates Q_{ent} were applied at the outlet of the device. The 2D entrainment geometry chosen in this work is shown in Fig. 4. This entrainment geometry is one of three

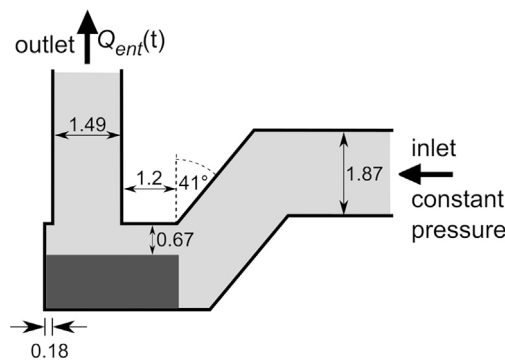


Fig. 4. The entrainment geometry used in this study (dimensions in mm). This is one of the optimized geometries found by Kopsch et al. (2016a). The area shaded in dark grey represents the initial distribution of drug powder.

optimized geometries found in our previous work (Kopsch et al., 2016a). It achieved low costs in terms of objective A, i.e. low patient-to-patient variability. Furthermore, it also achieved low costs in terms of objective B: to deliver an early bolus of drug.

ANSYS Meshing was used to mesh the geometry. The target cell size was 0.05 mm, which resulted in 8076 cells. The CFD solver settings for ANSYS Fluent that were used in this study are presented in Table 1. In previous studies (Kopsch et al., 2016a,b) it has been shown that these settings can produce results that are in good agreement with experimental results from Tuley et al. (2008) and are comparable to results achieved with a different CFD solver (OpenFOAM (The OpenFOAM Foundation, 2016)).

The outlet boundary conditions were transient inhalation flow rate profiles. When a flow rate profile Q_{ent} is applied at the outlet, the entrainment of drug powder in the compartment can be monitored as a function of time t . From the simulation the mass of drug released from the device, $M(t)$, was calculated as a function of time.

2.2.2. Predicting the entrainment behaviour with the meta-model

The aim was to use a finite number of CFD simulations to construct a simplified meta-model that is able to predict $M(t)$ for different $Q_{ent}(t)$. Once the meta-model is constructed, it may be used to predict $M(t)$ for different $Q_{ent}(t)$ without running further CFD simulations. Since the meta-model is only a simplified description of complex CFD entrainment simulations, it is not able to capture details of the fluid flow.

In this meta-model it is assumed that $\frac{dM}{dt}$, the rate of mass entrainment, may be modelled as a function of only two variables, the instantaneously applied flow rate Q_{ent} and the amount of drug remaining in the device (or, equivalently, the amount released from the device M). Thus

$$\frac{dM}{dt} = F(M, Q_{ent}) \quad (4)$$

In fact the exact mass flow rate of powder exiting the device at a particular time will depend on the exact distribution (i.e. volume fraction) and flow velocities of powder and air over the whole modelled domain at that particular instant. However, provided that Q_{ent} does not vary very rapidly compared to the transit time for flow through the domain and that the flow regime does not significantly change (as characterised by the Reynolds and Stokes numbers), the approximation of Eq. (4) is expected to be satisfactory for our purposes.

In order to estimate an approximate functional relationship $F(M, Q_{ent})$ the results of 20 CFD simulations have been used. In each of these CFD simulations a different constant flow rate Q_{ent} has been applied at the outlet, yielding different $M(t)$. As an illustration, Fig. 5a shows how two different constant inhalation flowrates Q_{ent} result in different release profiles $M(t)$. Fig. 5b shows the rate of drug release $\frac{dM}{dt}$ as a function of time. $\frac{dM}{dt}$ may also be expressed as a function of M , see Fig. 5c. The area shaded in grey

is the region in which values for the model $F(M, Q_{ent})$ can be interpolated from the results of these two CFD simulations.

In this study F has been approximated from the CFD results using a Python (Python Software Foundation, 2016) script. Bilinear interpolation was applied to predict values for $\frac{dM}{dt}$ for points (M, Q_{ent}) that lie between two curves. Bilinear interpolation was chosen because of its simplicity compared to other predictive modelling approaches. Once the numerical approximation for F is known Eq. (4), a differential equation, may be solved numerically to predict $M(t)$ for any specified flow rate profile $Q_{ent}(t)$. The Python library SciPy (The Scipy community, 2016) has been used to solve this equation numerically.

2.3. Optimization of the bypass ratio

Given a set of N measurements of inhalation profiles, the ratio of bypass to main entrainment flow r (see Eq. (3)) that best achieves a desired drug release behaviour is sought. This is an optimization problem. By systematically varying the parameter r it is hoped to minimize a cost function C that represents the degree to which desired drug release behaviour is achieved.

2.3.1. Optimization objective

For each inhalation flow rate measurement $Q_i(t)$ the meta-model described in Section 2.2 can predict the corresponding drug release profile $M_i(x)$. For many therapeutic applications it is desired to achieve an early bolus delivery of drug. Such a target release profile may be defined as

$$M_{target}(x) = \begin{cases} M_{tot} \frac{x}{x_0} & \text{if } x < x_0 \\ M_{tot} & \text{if } x \geq x_0 \end{cases} \quad (5)$$

This is a ‘ramp’ function that reaches total release of drug M_{tot} after a fraction x_0 of inhaled air volume. The optimization goal is to achieve drug release profiles $M_i(x)$ as close as possible to the target profile $M_{target}(x)$. We choose to measure the difference between $M_i(x)$ and $M_{target}(x)$ with the integral

$$C_i = \int_0^1 (M_i(x) - M_{target}(x))^2 dx \quad (6)$$

The total cost function is the average of all C_i for the N measured breath profiles:

$$C = \frac{1}{N} \sum_{i=1}^N C_i \quad (7)$$

The approach to calculate the cost function C is illustrated in Fig. 6. Fig. 6a shows $N=3$ inhalation flow rate profiles $Q_i(t)$ ($i=1, 2, 3$). Accordingly, Fig. 6b shows the resulting drug release profiles $M_i(x)$ and the target function $M_{target}(x)$. As an example, the area of the graph shaded grey shows the difference between Profile 1 and the target; this difference determines the value of the cost function C_1 .

Table 1
CFD solver settings for EE ANSYS Fluent (ANSYS, 2009) simulation.

CFD Modeling Parameter	Value or Model
Inlet boundary condition	Atmospheric pressure (101,325 Pa)
Outlet boundary condition	A transient flow rate profile $Q_{ent}(t)$
Granular viscosity model	‘Gidaspow’ (Gidaspow et al. (1992))
Frictional viscosity model	‘Johnson et al.’ (Johnson and Jackson (1987))
Granular temperature	‘Algebraic’
Solids pressure	‘Lun et al.’ (Ding and Gidaspow (1990), Lun et al. (1984))
Radial distribution	‘Lun et al.’ (Ding and Gidaspow (1990), Lun et al. (1984))
Drag coefficient	‘Gidaspow’ (Gidaspow et al. (1992))

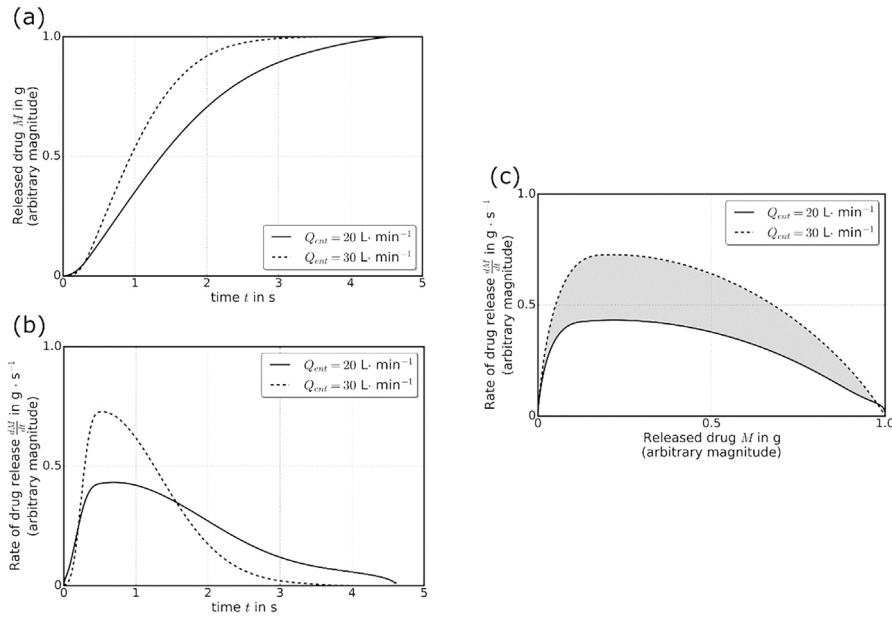


Fig. 5. Idealized representations of drug release M and the rate of drug release $\frac{dM}{dt}$ as functions of time t and of each other. Example data for clarification purposes only. (a) Two drug release profiles M as a function of time t for two different entrainment flow rates Q_{ent} . (b) The corresponding profiles of rate of drug release $\frac{dM}{dt}$ as a function of time t . (c) $\frac{dM}{dt}$ as a function of M for the same two profiles. The area between the two graphs is indicated in grey.

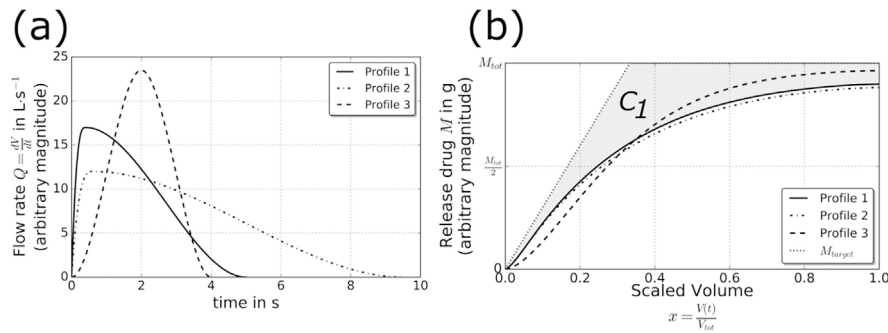


Fig. 6. Idealized representations of the process to calculate the cost function. Example data for clarification purposes only. (a) $N = 3$ inhalation flowrate profiles $Q_i(t)$. (b) The resulting mass release profiles $M_i(x)$ and the target release profile $M_{target}(x)$ for $x_0 = \frac{1}{3}$. The difference between M_1 and the target profile is shaded grey and determines the cost C_1 .

2.3.2. Optimization framework

Fig. 7 shows the method used to obtain the optimal ratio r of bypass to main entrainment flow. First, measurements of N different inhalation profiles $Q_i(t)$ of a specific patient are needed. Given a particular choice of the ratio r , and by applying the meta-model presented in Section 2.2, the drug release profiles $M_i(x)$ are then predicted for all inhalation profiles. Consequently, the cost function C (Eq. (7)) may be calculated. Next r is varied systematically, using a steepest gradient descent algorithm (Nocedal and Wright, 2006), to minimize C . When no further reductions of C can be achieved the result is considered to have converged and the corresponding value of r to be optimal.

3. Results

3.1. Validation of the meta-model approach

The EE CFD method used in this study has been partially validated in our previous work (Kopsch et al., 2016a; Zimarev et al., 2013). This was accomplished by comparing CFD results to experimental data, i.e. from Tuley et al. (2008), and to results

from another CFD solver: OpenFOAM (The OpenFOAM Foundation, 2016). For this reason, it was assumed that the chosen EE approach is able to generate realistic results. In order to construct the meta-model 20 EE CFD simulations with different constant inhalation flow rates Q_{ent} have been conducted for the entrainment geometry shown in Fig. 4. After the meta-model was constructed, its performance was tested using independent CFD results. Testing is important to ensure that (i) the complexity of the chosen model and (ii) the number of CFD simulations used to construct the model are sufficient to make reasonable predictions.

The goal of the meta-model was to express $\frac{dM}{dt}$ as a function of M and Q_{ent} , as described in Section 2.2. Fig. 8a shows the rate of drug entrainment $\frac{dM}{dt}$ as a function of drug released from the device M for five different (constant) flow rates. As shown in Fig. 8a the rate of entrainment $\frac{dM}{dt}$ tends to zero when the flow rate Q_{ent} is small and when most of the drug is released (i.e. when M approaches M_{tot}). This is expected, because drug cannot be entrained either at small flow rates or when no drug is left in the DPI compartment. The peaks observed in the $\frac{dM}{dt} - M$ plots represent occasions when a bolus of drug is released.

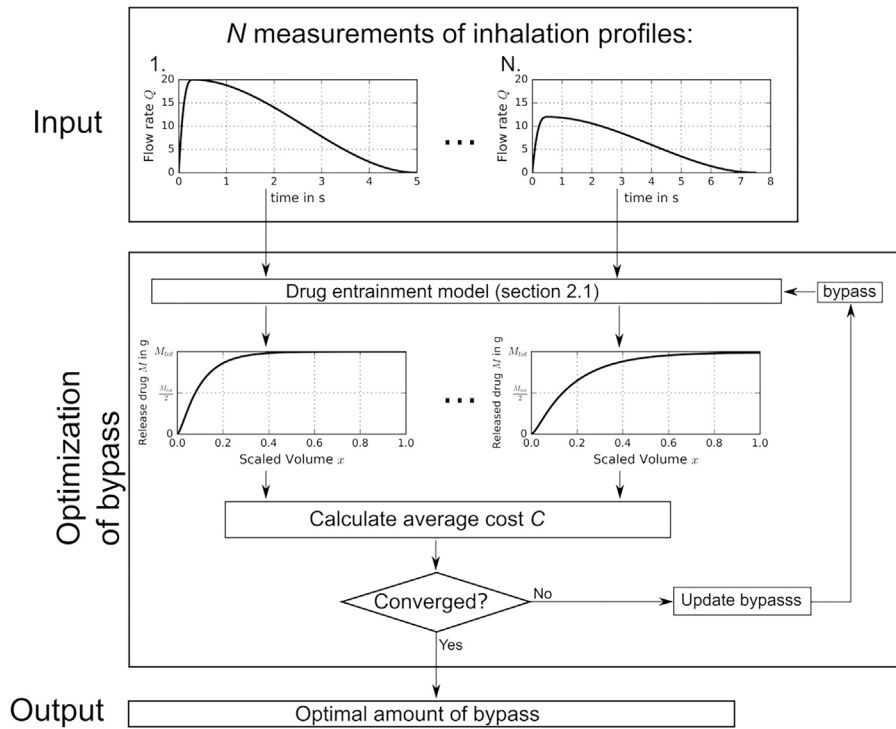


Fig. 7. The optimization framework uses N measurements of inhalation profile to predict the required amount of bypass.

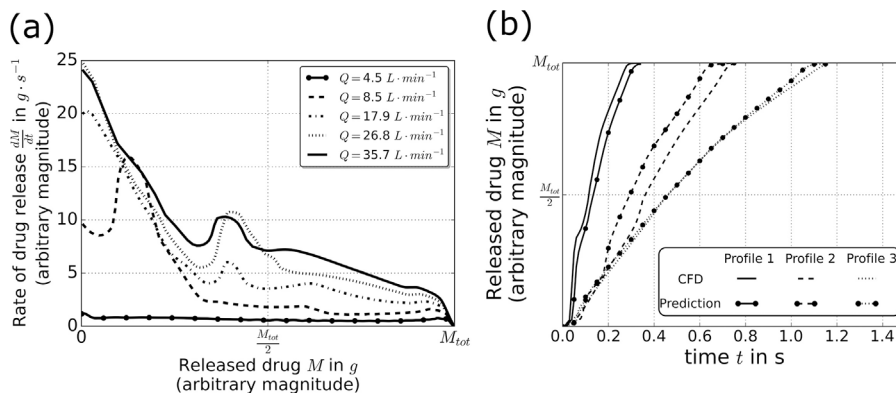


Fig. 8. (a) The rate of drug entrainment $\frac{dM}{dt}$ as a function of flow rate Q_{ent} and released mass of drug M . (b) Drug release as a function of time for three different inhalation profiles. The solid lines show CFD results, the dotted lines correspond to predictions made by the meta model.

Once the meta-model is constructed, it can be used to predict the drug released $M(t)$. The meta-model has been tested by predicting $M(t)$ profiles for new flow rate profiles $Q_{ent}(t)$ that were not previously used to construct the meta-model. These predictions were then compared to predictions made using new CFD simulations, see Fig. 8b. Fig. 8b shows reasonable agreement between the meta-model and new CFD simulations for the three cases tested. The agreement is especially good for profiles 1 and 3. If higher accuracy is needed, the meta-model may be refined further. This could be achieved by using more CFD simulations to construct the meta-model. The key advantage of the meta-model compared to CFD simulations is the saving of computation costs. While a typical CFD simulation takes around three hours to complete on a standard desktop personal computer, the meta-model can make a prediction within milliseconds.

In summary, the meta-model presented gives reasonable agreement with additional CFD simulations. Therefore it is considered appropriate to predict the release of drug in a DPI for different inhalation flow rate profiles.

3.2. Application of the bypass optimization approach

As an example, the optimization framework has been applied to calculate the optimal ratio r for two fictitious patients. Patient 1 can reach peak inspiratory flow rates between 60 and 80 $L \cdot min^{-1}$, see Fig. 9a. These flow rates are representative for healthy subjects or asthmatic patients with good lung function (de Koning et al., 2002; Persson et al., 1997; Tarsin et al., 2006). Patient 2 has poorer lung function, and can only achieve flow rates between 25 and 35 $L \cdot min^{-1}$, see Fig. 9b. Patient 2 represents a generic patient with

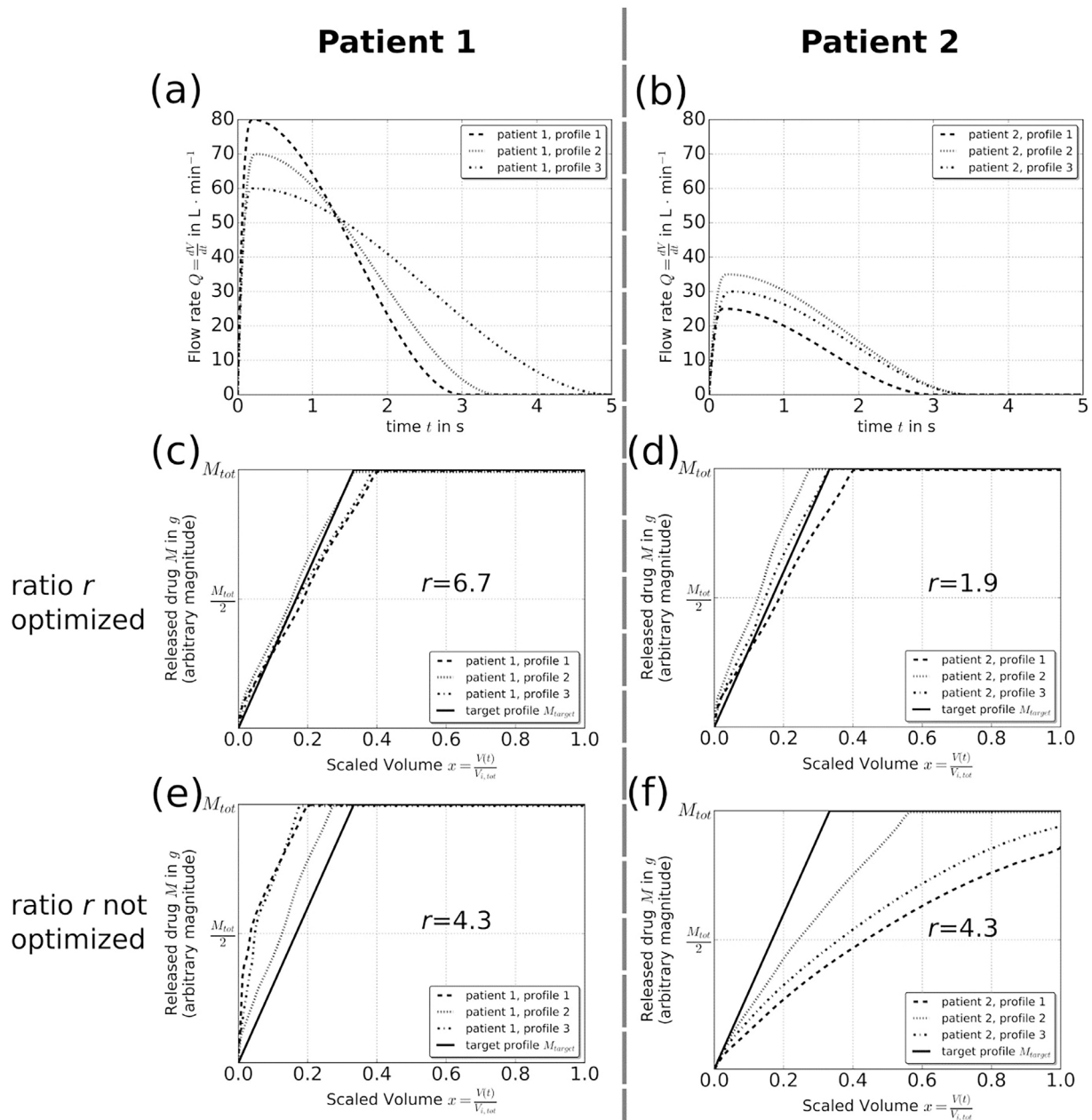


Fig. 9. Illustrative inhalation profiles: (a) Patient 1, with normal lung function; (b) Patient 2, with reduced lung function. The corresponding drug release profiles for different bypass-to-entrainment-flow ratios r : (c) Patient 1 with optimized $r=6.7$; (d) Patient 2 with optimized $r=1.9$; (e) Patient 1 with $r=4.3$; (f) Patient 2 with $r=4.3$.

reduced lung function, for example in elderly patients or in those with severe COPD (Al-showair et al., 2007; Broeders et al., 2001). The optimization algorithm was used to adjust r , the ratio of bypass to entrainment flow, for each patient to best achieve the desired target release behaviour. For patient 1 the optimized ratio was found to be $r=6.7$; for patient 2 the optimized ratio was found to be $r=1.9$. Fig. 9c and d show the release profiles with the optimized bypass for patient 1 and 2 respectively. For comparison, Fig. 9e and f show the release profiles when the same, non-optimized, ratio $r=4.3$ is chosen for both patients (a 'one size fits all' approach). For this choice of r good agreement with the target profile M_{target} could not be achieved: for patient 1 (high lung function) drug powder is released too early, for patient 2 (low lung function) drug powder is released too late.

4. Discussion & conclusions

In summary, an optimization method has been developed to identify the optimal amount of bypass needed in a DPI for a particular patient. This method relies on a computational meta-model that can predict drug release from a device accurately. Compared to a high-fidelity CFD modelling approach the meta-model approach presented in this study can obtain results up to a million times faster. Consequently, it can easily be used as part of a bypass optimization process in which a large number of predictions have to be made.

The effectiveness of the optimization method has been shown by means of a numerical study. By identifying the optimal amount of bypass for particular patients a close match between drug

release profiles and a desired target release profile was obtained. This optimization method may be applied to develop a DPI with a settable amount of bypass.

Acknowledgment

T.K. was funded by an EPSRC Ph.D. studentship (EP/M506485/1). Data relating to this publication is available in Kopsch et al. (2017).

References

- ANSYS, ANSYS, I., 2009. Ansys. .
- Al-showair, R.A.M., Tarsin, W.Y., Assi, K.H., Pearson, S.B., Chrystyn, H., 2007. Can all patients with COPD use the correct inhalation flow with all inhalers and does training help? *Respir. Med.* 2395–2401. doi:http://dx.doi.org/10.1016/j.rmed.2007.06.008.
- Broeders, M.E.A.C., Molema, J., Vermue, N.A., Folgering, H.T.M., 2001. Peak inspiratory flow rate and slope of the inhalation profiles in dry powder inhalers. *Eur. Respir. J.* 18, 780–783. doi:http://dx.doi.org/10.1183/09031936.01.00240301.
- Chen, L., Heng, R., Admasu, M., Cai, J., Du, D., Linus, U., 2013. Investigation of dry powder aerosolization mechanisms in different channel designs. *Int. J. Pharm.* 457, 143–149. doi:http://dx.doi.org/10.1016/j.ijpharm.2013.09.012.
- Coates, M.S., Chan, H.-K., Fletcher, D.F., Raper, J.A., 2006. Effect of design on the performance of a dry powder inhaler using computational fluid dynamics. Part 2: air inlet size. *J. Pharm. Sci.* 95, 1382–1392. doi:http://dx.doi.org/10.1002/jps.20603.
- de Koning, J.P., van Der Mark, T.W., Coenegracht, P.M.J., Tromp, T.F.J., Frijlink, H.W., 2002. Effect of an external resistance to airflow on the inspiratory flow curve. *Int. J. Pharm.* 234, 257–266. doi:http://dx.doi.org/10.1016/S0378-5173(01)00969-3.
- Ding, J., Gidaspow, D., 1990. A bubbling fluidization model using kinetic theory of granular flow. *AIChE J.* 36, 523–538. doi:http://dx.doi.org/10.1002/aic.690360404.
- Ehtezazi, T., Allanson, D.R., Jenkinson, I.D., Shrubbs, I., O'Callaghan, C., 2008. Investigating improving powder deagglomeration via dry powder inhalers at a low inspiratory flow rate by employing add-on spacers. *J. Pharm. Sci.* 97, 5212–5221. doi:http://dx.doi.org/10.1002/jps.21375.
- Gidaspow, D., Bezburuah, R., Ding, J., 1992. Hydrodynamics of circulating fluidized beds: kinetic theory approach. *Proceedings of the Seventh Engineering Foundation Conference on Fluidization* 75–82.
- Heyder, J., 2004. Deposition of inhaled particles in the human respiratory tract and consequences for regional targeting in respiratory drug delivery. *Proc. Am. Thorac. Soc.* 1, 315–320. doi:http://dx.doi.org/10.1513/pats.200409-046TA.
- Johnson, P.C., Jackson, R., 1987. Frictional-collisional constitutive relations for granular materials, with application to plane shearing. *J. Fluid Mech.* 176, 67. doi:http://dx.doi.org/10.1017/S0022112087000570.
- Kopsch, T., Symons, D., Murnane, D., 2015. Design-optimization of dry powder inhalers: selecting an objective function. DDL26 Conference. .
- Kopsch, T., Murnane, D., Symons, D., 2016a. Optimizing the entrainment geometry of a dry powder inhaler: methodology and preliminary results. *Pharm. Res.* 33, 2668–2679. doi:http://dx.doi.org/10.1007/s11095-016-1992-3.
- Kopsch, T., Symons, D., Murnane, D., 2016b. Modelling drug entrainment in a dry powder inhaler: benchmarking and sensitivity analysis of a multiphase CFD approach. DDL27 Conference. .
- Kopsch T., Murnane D., Symons D., 2017., Supporting material. URL <https://doi.org/10.17863/CAM.11804>
- Lun, C.K.K., Savage, S.B., Jeffrey, D.J., Chepurini, N., 1984. Kinetic theories for granular flow: inelastic particles in couette flow and slightly inelastic particles in a general flowfield. *J. Fluid Mech.* 140, 223–256. doi:http://dx.doi.org/10.1017/S0022112084000586.
- Milenkovic, J., Alexopoulos a, a.H., Kiparissides, C., 2014. Deposition and fine particle production during dynamic flow in a dry powder inhaler: a CFD approach. *Int. J. Pharm.* 461, 129–136. doi:http://dx.doi.org/10.1016/j.ijpharm.2013.11.047.
- Nocedal, J., Wright, S.J., 2006. Numerical Optimization, Springer Series in Operations Research and Financial Engineering. Springer, New York doi:http://dx.doi.org/10.1007/978-0-387-40065-5.
- Persson, G., Olsson, B., Soliman, S., 1997. The impact of inspiratory effort on inspiratory flow through Turbuhaler[®] in asthmatic patients. *Eur. Respir. J.* 681–684. doi:http://dx.doi.org/10.1183/09031936.97.10030681.
- Python Software Foundation, 2016. Python Language Reference, Version 2.7.6. .
- Tarsin, W.Y., Pearson, S.B., Assi, K.H., Chrystyn, H., 2006. Emitted dose estimates from Seretide[®] Diskus[®] and Symbicort[®] Turbuhaler[®] following inhalation by severe asthmatics. *Int. J. Pharm.* 316, 131–137. doi:http://dx.doi.org/10.1016/j.ijpharm.2006.02.040.
- The OpenFOAM Foundation, 2016. OpenFOAM 2.4. . <http://www.openfoam.org/>.
- The Scipy community, 2016. SciPy Python Library Documentation, Version 0.17.1. . <http://docs.scipy.org/doc/scipy/reference/>.
- Tong, Z.B., Zheng, B., Yang, R.Y., Yu, a.B., Chan, H.K., 2013. CFD-DEM investigation of the dispersion mechanisms in commercial dry powder inhalers. *Powder Technol.* 240, 19–24. doi:http://dx.doi.org/10.1016/j.powtec.2012.07.012.
- Tuley, R., Shrimpton, J., Jones, M.D., Price, R., Palmer, M., Prime, D., 2008. Experimental observations of dry powder inhaler dose fluidisation. *Int. J. Pharm.* 358, 238–247. doi:http://dx.doi.org/10.1016/j.ijpharm.2008.03.038.
- Wong, W., Fletcher, D.F., Traini, D., Chan, H.K., Crapper, J., Young, P.M., 2010. Particle aerosolisation and break-up in dry powder inhalers 1: evaluation and modelling of venturi effects for agglomerated systems. *Pharm. Res.* 27, 1367–1376. doi: <http://dx.doi.org/10.1007/s11095-010-0128-4>.
- Wong, W., Fletcher, D.F., Traini, D., Chan, H.-K., Crapper, J., Young, P.M., 2011a. Particle aerosolisation and break-up in dry powder inhalers: evaluation and modelling of the influence of grid structures for agglomerated systems. *J. Pharm. Sci.* 100, 4710–4721. doi:http://dx.doi.org/10.1002/jps.22663.
- Wong, W., Fletcher, D.F., Traini, D., Chan, H., Crapper, J., Young, P.M., 2011b. Particle aerosolisation and break-up in dry powder inhalers: evaluation and modelling of impaction effects for agglomerated systems. *J. Pharm. Sci.* 100, 2744–2754. doi:http://dx.doi.org/10.1002/jps.22503.
- Zimarev, D., Parks, G., Symons, D., 2013. Computational modelling and stochastic optimisation of entrainment geometries in dry powder inhalers. DDL24 Conference. .